HAL
open science

Stabilizing role of structural elements within the 5´ Untranslated Region (UTR) and gag sequences in Mason-Pfizer monkey virus (MPMV) genomic RNA packaging

Rawan Kalloush, Valérie Vivet-Boudou, Lizna Ali, Vineeta Pillai, Farah Mustafa, Roland Marquet, Tahir Rizvi

To cite this version:

Rawan Kalloush, Valérie Vivet-Boudou, Lizna Ali, Vineeta Pillai, Farah Mustafa, et al.. Stabilizing role of structural elements within the 5´ Untranslated Region (UTR) and gag sequences in Mason-Pfizer monkey virus (MPMV) genomic RNA packaging. RNA Biology, 2019, 16 (5), pp.612-625. 10.1080/15476286.2019.1572424 . hal-02119053

HAL Id: hal-02119053

https://cnrs.hal.science/hal-02119053v1

Submitted on 30 May 2020

HAL is a multi-disciplinary open access archive for the deposit and dissemination of scientific research documents, whether they are published or not. The documents may come from teaching and research institutions in France or abroad, or from public or private research centers.

L'archive ouverte pluridisciplinaire **HAL**, est destinée au dépôt et à la diffusion de documents scientifiques de niveau recherche, publiés ou non, émanant des établissements d'enseignement et de recherche français ou étrangers, des laboratoires publics ou privés.

RNA Biology

ISSN: 1547-6286 (Print) 1555-8584 (Online) Journal homepage: https://www.tandfonline.com/loi/krnb20

Stabilizing role of structural elements within the 5´ Untranslated Region (UTR) and gag sequences in Mason-Pfizer monkey virus (MPMV) genomic RNA packaging

Rawan M. Kalloush, Valérie Vivet-Boudou, Lizna M. Ali, Vineeta N. Pillai, Farah Mustafa, Roland Marquet & Tahir A. Rizvi

To cite this article: Rawan M. Kalloush, Valérie Vivet-Boudou, Lizna M. Ali, Vineeta N. Pillai, Farah Mustafa, Roland Marquet & Tahir A. Rizvi (2019) Stabilizing role of structural elements within the 5´ Untranslated Region (UTR) and gag sequences in Mason-Pfizer monkey virus (MPMV) genomic RNA packaging, RNA Biology, 16:5, 612-625, DOI: 10.1080/15476286.2019.1572424

To link to this article: https://doi.org/10.1080/15476286.2019.1572424

View supplementary material

Published online: 17 Feb 2019.

Submit your article to this journal

Article views: 45

View Crossmark data

Full Terms & Conditions of access and use can be found at
https://www.tandfonline.com/action/journalInformation?journalCode=krnb20

RNA BIOLOGY
2019, VOL. 16, NO. 5, 612–625
https://doi.org/10.1080/15476286.2019.1572424

Taylor & Francis
Taylor & Francis Group

RESEARCH PAPER

Check for updates

Stabilizing role of structural elements within the 5´ Untranslated Region (UTR) and gag sequences in Mason-Pfizer monkey virus (MPMV) genomic RNA packaging

Rawan M. Kalloush[a*], Valérie Vivet-Boudou [b*], Lizna M. Ali[a], Vineeta N. Pillai[a], Farah Mustafa [c], Roland Marquet[b], and Tahir A. Rizvi[a]

[a]Department of Microbiology & Immunology College of Medicine and Health Sciences, United Arab Emirates University, Al Ain, United Arab Emirates (UAE); [b]CNRS, Architecture et Réactivité de l'ARN, UPR, Université de Strasbourg, Strasbourg, France; [c]Department of Biochemistry, College of Medicine and Health Sciences, United Arab Emirates University, Al Ain, United Arab Emirates (UAE)

ABSTRACT

The Mason-Pfizer monkey virus (MPMV) genomic RNA (gRNA) packaging signal is a highly-structured element with several stem-loops held together by two phylogenetically conserved long-range interactions (LRIs) between U5 and *gag* complementary sequences. These LRIs play a critical role in maintaining the structure of the 5´ end of the MPMV gRNA. Thus, one could hypothesize that the overall RNA secondary structure of this region is further architecturally held together by three other stem loops (SL3, Gag SL1, and Gag SL2) comprising of sequences from the distal parts of the 5´untranslated region (5′ UTR) to ~ 120 nucleotides into *gag*, excluding *gag* sequences involved in forming the U5-Gag LRIs. To provide functional evidence for the biological significance of these stem loops during gRNA encapsidation, these structural motifs were mutated and their effects on MPMV RNA packaging and propagation were tested in a single round *trans*-complementation assay. The mutant RNA structures were further studied by high throughput SHAPE (hSHAPE) assay. Our results reveal that sequences involved in forming these three stem loops do not play crucial roles at an individual level during MPMV gRNA packaging or propagation. Further structure–function analysis indicates that the U5-Gag LRIs have a more important architectural role in stabilizing the higher order structure of the 5´ UTR than the three stem loops which have a more secondary and perhaps indirect role in stabilizing the overall RNA secondary structure of the region. Our work provides a better understanding of the molecular interactions that take place during MPMV gRNA packaging.

ARTICLE HISTORY
Received 31 December 2018
Accepted 17 January 2019

KEYWORDS
Retroviruses; Mason-Pfizer monkey virus (MPMV); RNA packaging; RNA secondary structure; gag; U5/Gag LRIs

Introduction

Packaging of retroviral genomic RNA (gRNA) is one of the essential steps in retroviral replication during which two copies of 'full length' unspliced gRNA are selectively encapsidated into the assembling virus particles from a large *milieu* of cellular and viral RNAs in the host cell cytoplasm [1–8]. Specific encapsidation involves recognition of particular sequence(s) of the gRNA located at its 5´-end, termed psi (ψ), or the 'packaging signal' [1–3,5–7,9]. The specific capture of the ψ-containing gRNAs by the assembling virions requires the interaction of ψ with the zinc finger motifs of the nucleocapsid (NC) domain of the viral Gag polyprotein [1–3,5–7,9]. For all retroviruses studied so far, determinants of gRNA packaging map to the first ~100 to 400 nucleotides (nts) at the 5´end of the gRNA [1–3,5–7].

The Mason-Pfizer monkey virus (MPMV) is a *betaretrovirus* and a prototype of type-D retrovirus that has been implicated in causing an immunodeficiency syndrome in newly borne rhesus monkeys [10,11]. Several other retroviruses that are similar to MPMV such as simian retrovirus types 1 and 2 (SRV-1 and −2) have also been identified which cause immunodeficiency syndrome [12–14]. Within the Type-D retroviruses, MPMV has been investigated the most in terms of its overall biology and replication with special emphasis on gRNA packaging, dimerization, and RNA propagation [15–24]. This is partly because MPMV-based vectors are being considered as tools for gene therapy since: i) MPMV promoter is transcriptionally active in human cells- a prerequisite for human gene therapy, and ii) therapeutic genes may require nuclear export signals like the MPMV constitutive transport element (CTE) for their efficient expression in the target cells [16,25–27].

A systematic deletion analysis of the 5´end of the MPMV genome has suggested that a discontinuous region in the 5´untranslated region (UTR) in conjunction with the first 100 nts of *gag* are critical for MPMV gRNA packaging [19,21,22]. Later, employing a combination of structural, phylogenetic, biochemical, and genetic analyses, it has been shown that MPMV packaging determinants (5´ UTR and beginning of *gag*) fold into a complex RNA structure comprising of several stable stem loops [15,19]. A distinguishing feature of the predicted and the selective

CONTACT Tahir A. Rizvi tarizvi@uaeu.ac.ae Department of Microbiology & Immunology, CMHS, UAEU, P.O. Box 17666, Al Ain, UAE; Roland Marquet r.marquet@ibmc-cnrs.unistra.fr CNRS, Architecture et Réactivité de l'ARN, Université de Strasbourg, UPR 9002, IBMC, 15 rue René Descartes, Strasbourg cedex 67084, France; Farah Mustafa fmustafa@uaeu.ac.ae Department of Biochemistry, CMHS, UAEU, P.O. Box 17666, Al Ain, UAE
*These authors contributed equally to this work.
Supplemental data for this article can be accessed here.

© 2019 Informa UK Limited, trading as Taylor & Francis Group

2′ hydroxyl acylation primer extension (SHAPE)-validated structure is the presence of U5-Gag long range interactions (LRIs), a stretch of single-stranded purine (ssPurine)-rich region, and a characteristic G-C-rich palindromic (pal) stem loop (pal SL: Fig. 1A [15,20]). Deletion and substitution analysis of sequences comprising these structural motifs has shown that the principal packaging and dimerization determinants of MPMV lie within Region A, the palSL, ssPurines, and Region B – an area that contains a partial repeat of ssPurine [15,19,22]. Flanking the LRIs, at

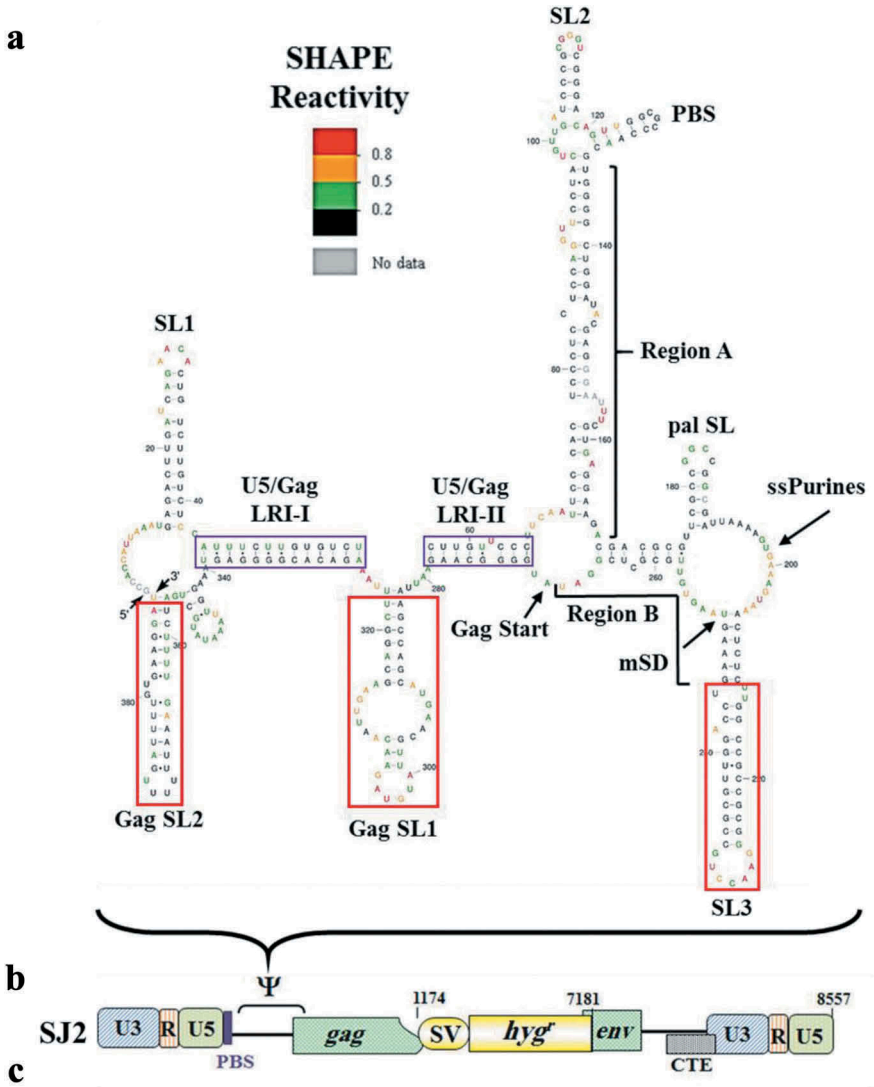

Clone Name	Description of the Mutations
RK15	Deletion of 33 nts (of 43 nts) of SL3
RK16	Deletion of 30 nts of Gag SL2
RK17	Deletion of 39 nts of Gag SL1
RK18	Double Deletion of SL3 and Gag SL1
RK19	Double Deletion of SL3 and Gag SL2
RK20	Double Deletion of Gag SL1 and Gag SL2
RK21	Exchange of Gag SL1 and Gag SL2
RK22	Triple Deletion of SL3, Gag SL2 and Gag SL1

Figure 1. Effect of deletion mutations introduced into sequences at the 3´ end of the SHAPE-validated structure forming SL3, Gag SL1, and Gag SL2 on RNA packaging and propagation. (a) Illustration of the SHAPE-validated structure of MPMV packaging signal RNA with SL3, Gag SL1, and Gag SL2 highlighted in red boxes. The other important sequence and structural elements present in this region, SL1, SL2, PBS, pal SL, ssPurines, major splice donor (mSD), LRI I, and LRI II are also highlighted in different color codes. Part of the figure adapted from Aktar et al [15]. **(b)** Schematic representation of the MPMV wild type sub-genomic transfer vector, SJ2 [19], in which the region between R and 120 nts of Gag that has been shown to be important for MPMV RNA packaging and dimerization is demarcated. The same region was used to predict and validate the RNA secondary structure. **(c)** Table describing the mutants tested in this study.

the 5′ end of the packaging signal are two conserved stem loops, SL1 and SL2. No specific function has been attributed to SL1 in the viral life cycle despite its conservation among five different strains of MPMV [15], though it may serve to anchor the whole 5′ UTR structure since it is the first stem loop observed at the 5′ end of the viral genome. On the other hand, SL2 represents a long and stable stem loop that has characteristically been observed in other retroviruses such as human, simian, and feline immunodeficiency viruses (HIV, SIV, and FIV) [28-33], and mouse mammary tumor virus (MMTV) [34]. It contains the primer binding site (PBS) of the virus as well as Region 'A' which is part of the principal packaging determinant of MPMV [15,19,22].

In addition, there are 3 distinct stem loops (SL3, Gag SL1 and Gag SL2) at the 3′ end of the packaging signal RNA, out of which SL3 is exclusively comprised of 5′ UTR sequences, whereas Gag SL1 and Gag SL2 are formed employing sequences solely from *gag* (Fig. 1A [15,19,20]). Sequences within *gag* have been universally shown to be involved in gRNA packaging among retroviruses [1–3,5,6,9], but it is not clear what their actual role may be in this process. The crucial role(s) of ssPurine-rich region, pal SL, and U5-Gag LRIs during MPMV gRNA packaging and dimerization have already been established by genetic, biochemical, and structure-function analyses [15,19,20]. However, the role of sequences forming SL3, Gag SL1 and Gag SL2 at either the sequence or structural levels has not been tested genetically, although it may offer a possible mechanistic elucidation for the multipartite nature of MPMV packaging determinants [19].

Therefore, to establish the biological significance of these structural motifs and to provide functional evidence for their existence, a number of deletion and substitutions mutations were introduced in the sequences involved in forming SL3, Gag SL1, and Gag SL2 and tested in a biologically relevant *in vivo* packaging and transduction assay to determine their effects on MPMV gRNA packaging and propagation. Furthermore, in order to perform a complete structure-function analysis, the structures of the mutated RNAs were analyzed by *in vitro* hSHAPE chemical probing. Our results reveal that the three stem loops are not directly involved in the gRNA packaging process, but may be important for stabilizing the overall RNA structure of the 5′ end of the viral genome. This observation sheds further light on the primarily stabilizing effect of the *gag* sequences towards the packaging potential of retroviral gRNA.

Results and discussion

Experimental strategy for packaging and propagation assays

The sequences involved in formation of the SL3, Gag SL1, and Gag SL2 fall in a region that includes sequences extending into *gag* [15,19,22]. Therefore, it is difficult to test the effects of mutations in this region in the full-length genomic context as these mutations would disrupt Gag/Pol protein synthesis. To overcome such a caveat, we used our well-established three-plasmid *trans*-complementation assay developed to study MPMV RNA packaging [35] (Fig. 2). The assay provides the necessary biological components to generate virus particles containing packaged RNAs, the replication of which is limited to a single round because re-infection of the target cells cannot take place [35] (Fig. 2). Briefly, the Gag and Gag/Pol proteins were provided in *trans* from an MPMV expression plasmid (TR301), while heterologous envelope proteins were provided by the envelope expressing plasmid (MD.G) encoding the vesicular stomatitis G protein (VSV-G [36]), leading to the generation of MPMV virions capable of packaging competent RNA substrates (Fig. 2A). These plasmids were co-transfected with either the wild type (SJ2; Fig. 1B [19]) or mutant transfer vectors (Figs. 1C and 2B) providing the RNA substrates for packaging. Presence of hygromycin resistance gene on the transfer vector RNAs allowed the monitoring of packaged RNA propagation into the target cells. Co-transfection of a firefly *luciferase* expression plasmid (pGL3C) along with these plasmids into the producer 293T cells allowed estimation of the transfection efficiency. Following *trans* complementation, the newly formed virus particles were used to quantify the amount of packaged RNA (Fig. 2C) and monitor its propagation into the infected HeLa T4 cells following transduction of the infected HeLa T4 cells via the marker hygromycin resistance gene (Fig. 2D). The propagation of the packaged RNA (number of resulting hygromycin resistant colonies) should be proportional to the amount of the packaged RNA. A previously designed custom-made qPCR assay was used for the quantitation of wild type or mutant MPMV RNAs [20]. This assay employs primers and probes in a region common to both the wild type and mutant RNAs (nts 702–770; see Supplemental Table 1 for primers and probe details), ensuring perfect complementarity with all target RNAs [20]. Finally, a commercially-available human β-actin assay was used as an endogenous control, as described previously [20,34,37,38].

Individually SL3, Gag SL1, and Gag SL2 are not important at either the sequence or structural level for MPMV RNA packaging and propagation

The SHAPE-validated structure of the 5′end of the MPMV genome (Fig. 1A) reveals that the secondary structure of the 5′ UTR sequences appears to be anchored by complementary U5 and Gag sequences forming the two LRIs, while sequences from the distal parts of the 5′ UTR and *gag* (but excluding the *gag* sequences involved in forming U5-Gag LRIs) form three stem loops (SL3, Gag SL1, and Gag SL2). In order to evaluate if these sequences (by virtue of forming SL3, Gag SL1, and Gag SL2 structural motifs) provide stability to the overall RNA secondary structure of the 5′-end of the MPMV genome, or directly act in the RNA packaging process, a systematic deletion/substitution analysis was performed, starting with single deletion of each of the stem loop structures (Fig. 1C). The RK15 mutant contained a 33-nucleotide deletion (from the distal part of the 5′ UTR), removing most of the sequences forming SL3, except for 10 nts in the basal part of SL3 stem (boxed region in Fig. 1A). This deletion carefully avoided the nucleotides associated with region 'B' as this region has

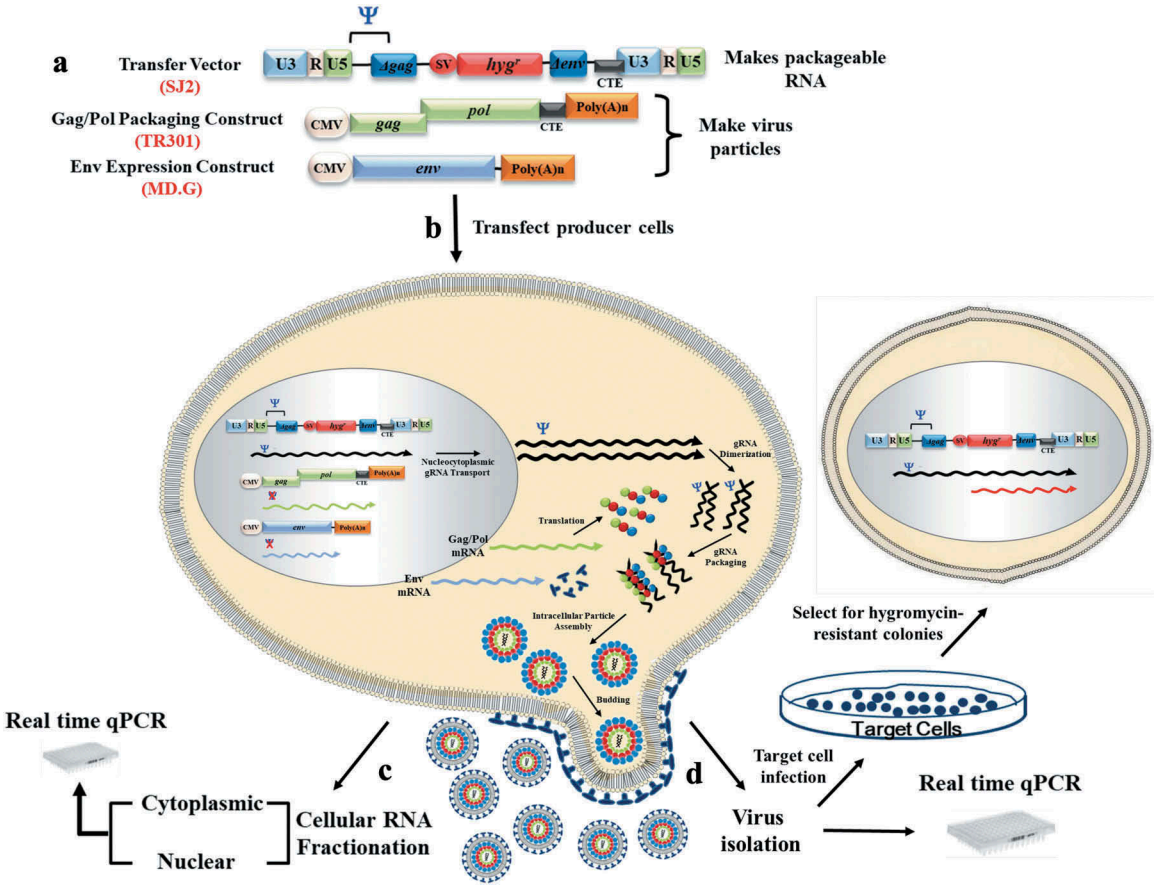

Figure 2. Illustration of the 3-plasmid *in vivo* packaging and propagation assay. (a) Graphical representation of the three plasmids used to produce virus particles. Gag/Pol structural proteins were produced by TR301, the packageable RNA substrate was produced by the wild type transfer vector, SJ2, while the vesicular stomatitis envelope glycoprotein to pseudotype the virus particles was produced by MD.G. **(b)** Schematic depiction of a 293T cell co-transfected with the three plasmids to produce infectious virus particles, which can only replicate to a single round. Unspliced RNA generated from the wild type vector, SJ2, can only be packaged into the virions owing to the presence of intact packaging signal. **(c)** 293T cells co-transfected with the three plasmids produce infectious virions and are fractionated into nuclear and cytoplasmic fractions. The cytoplasmic fractions are analyzed for functional RNA transport and expression. **(d)** Viral particles produced are tested for the amount of RNA packaged by real time PCR. Viral supernatants are also used to infect target cells (HeLa T4) to study RNA propagation. After infection, target cells are selected with media containing hygromycin B, allowing only those cells to survive which have been successful infected since the packaged RNA contains the *hygromycin resistance* gene cassette. Part of the figure adapted from Pitchai et al [68].

been shown to be critical for RNA packaging [19,22]. RK16 contained a 30-nucleotide deletion removing Gag SL2, while RK 17 had a 39-nucleotide deletion removing Gag SL1 (boxed regions in Fig. 1A).

These mutant transfer vector RNAs were tested in the *in vivo* packaging and propagation assay (Fig. 2) to assess the effects of the introduced mutations on MPMV gRNA packaging and propagation. The transfected 293T cells were fractionated into nuclear and cytoplasmic fractions and virions produced in the supernatant were pelleted by ultracentrifugation. Next, RNAs were extracted from both the cytoplasmic fractions and the pelleted viral particles and analyzed by RT PCR for the integrity of fractionation and MPMV expression (Fig. 2C). The purified cytoplasmic and virion RNAs were subjected to DNase-treatment to eliminate any contaminating plasmid DNA that may have been carried over from the transfected cultures. This was followed by confirming absence of plasmid DNA in the RNA preparations by transfer vector-specific PCR (oligos OTR 1161 and OTR 1163; **Table S1**). A lack of any demonstrable amplification in the DNase-treated RNAs revealed that the plasmid DNA contamination, if any, in these RNA preparations was below the detection level (Fig. 3A, panels I & II).

Next, PCRs were conducted on the cytoplasmic cDNAs to confirm that no RNA physically leaked from the nucleus to the cytoplasm during the fractionation process. This was accomplished by testing for the presence of unspliced β-actin mRNA in the cytoplasmic fractions, an mRNA that should remain exclusively nuclear, while the spliced β-actin mRNA should be observed in both the fractions. PCR analysis of cytoplasmic cDNAs (using oligos OTR 581 and OTR 582; **Table S1**) revealed that the unspliced β-actin mRNA could not be detected in any of the samples even though it could be detected in the nuclear fraction, which also served as a positive control (Fig. 3A, panels III). PCRs for the unspliced β-actin were conducted in a multiplex reaction along with primers/competimer for 18S rRNA to ensure that amplifiable cDNAs were present in these PCR reactions (Fig. 3A, panel III). Successful amplification of 18S rRNA, but absence of any amplifiable signal for unspliced β-actin mRNA suggested that the nuclear membrane integrity was not compromised during fractionation and that our RNA preparations were indeed cytoplasmic (Fig. 3A, panel III). The spliced β-actin PCRs

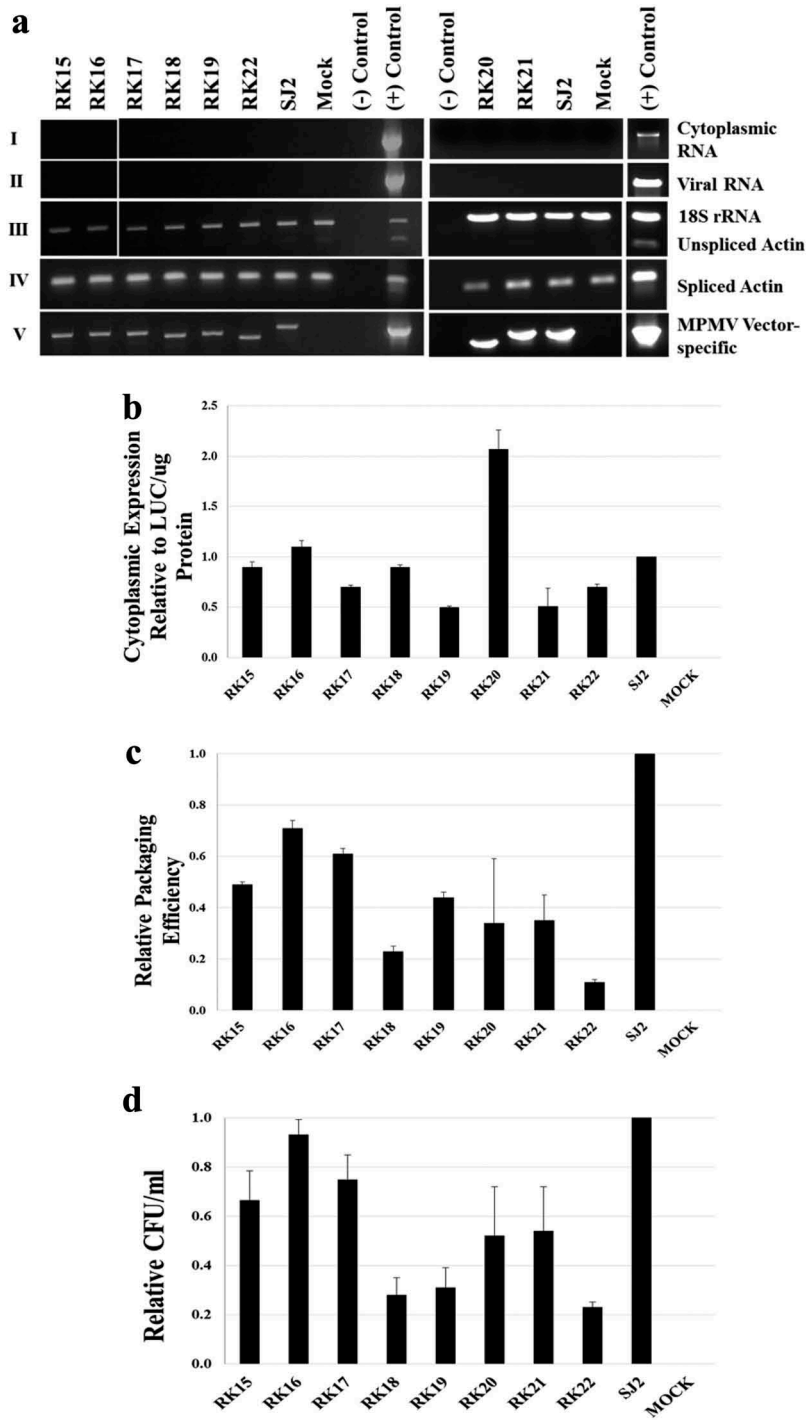

Figure 3. **Effect of deletion mutations introduced into sequences at the 3´ end of the SHAPE-validated structure of MPMV forming SL3, Gag SL1, and Gag SL2 on RNA packaging and propagation. (a)** Gel images of the controls needed for validating different aspects of the three plasmid *trans* complementation assay from one experiment for which the qPCR analysis was also conducted that is shown in panels B and C. This analysis was performed for each of the several independent experiments conducted to analyze the test constructs. The gels have been spliced together (as indicated by vertical white spaces) in different panels to create part A. **Panel (I)** PCR amplification of RNA preparations with MPMV-specific primers following DNase treatment from the cytoplasmic fractions, and **Panel (II)** viral particles. **Panel (III)** Multiplex PCR amplification for unspliced β-actin mRNA and 18S rRNA to check for the nucleocytoplasmic fractionation technique and amplifiability of the cDNAs. **Panel (IV)** PCR amplification of spliced β-actin mRNA. **Panel (V)** Transfer vector cytoplasmic cDNAs amplification using MPMV-specific primers. The positive control used for 18S rRNA, unspliced and spliced actin was gDNA, while the control in the remaining panels was the wild type (SJ2) plasmid DNA. **(b)** qPCR analysis of the cytoplasmic expression of transfer vector RNAs from producer 293T cells relative to the wild type (SJ2 vector) after normalization with the β-actin endogenous control and luciferase expression. The error bars represent the standard deviation (SD) of triplicates of each clone from a representative experiment (same as that shown in panel (**a**)) of several experiments conducted. **(c)** Relative RNA packaging efficiencies of mutant transfer vector RNAs compared to the wild type (SJ2) was measured by qPCR following normalization with cytoplasmic RNA expression of the corresponding mutants. The data shown is from a representative experiment (same as that shown in panel (**a**)) of several experiments conducted. **(d)** Relative propagation efficiencies of mutant transfer vector RNAs as measured by the hygromycin resistant colony-forming units (CFU)/ml relative to the wild type (SJ2) vector. The data represented in histograms correspond to the mean of samples in triplicates (± SD) from several experiments.

(using oligos OTR 580 and OTR 581; **Table S1**), on the other hand, showed, specific signal in all the cytoplasmic fractions (Fig. 3A, panel IV). Once confirmed, PCRs using MPMV-specific oligos (OTR 1161 and OTR 1163; **Table S1**) were conducted across the mutated regions to check proper expression and transport of the transfer vector RNAs to the cytoplasm. As can be seen, PCR amplified products were visible across the samples that varied in size depending upon the extent and location of the deletion relative to the primers used for the amplification, revealing that the transfer vector RNAs were stably expressed and properly transported to the cytoplasm (Fig. 3A, panel V and Fig. 3B).

We next analyzed the packaging efficiencies of the transfer vector RNAs transcribed from RK15-RK17 into viral particles relative to the wild type (SJ2) transfer vector RNA. Towards this end, the MPMV custom-designed real time qPCR assay was used in combination with a commercially available β-actin Taqman assay as an endogenous control on both the cytoplasmic and virion RNA samples in triplicates, as described earlier [20]. The ratio of the packaged mutant RNA was calculated compared to the wild type RNA to determine the relative packaging efficiency (RPE) of each mutant transfer vector RNA (Fig. 3C). This analysis revealed packaging efficiencies of 0.49, 0.71, and 0.61 for RK15, RK16, and RK17, respectively, compared to the WT construct, SJ2 (Fig. 3C). Among these, the RPE of only the SL3 deletion mutant (RK15) was significantly different from the WT (p value < 2.00E-4) compared to the constructs with Gag SL1, and Gag SL2 deletions. Next, the RNA propagation phenotype in these mutants was quantified by counting the hygromycin-resistant colonies (colony forming unit/ml; CFU/ml) that appeared in the transduced HeLa T4 cells following infection with the virus particles containing the hygromycin resistance gene on packaged transfer vector RNA (Fig. 2). In agreement with the RNA packaging data, the RNA propagation of these constructs was correspondingly reduced, though none of them reached statistically significant differences (Fig. 3D). The fact that only marginal effects on RNA packaging for one mutant and none for the RNA propagation potential of the transfer vector RNAs were observed despite the large deletions introduced in this region suggests that sequences involved in forming SL3, Gag SL1, or Gag SL2 do not play a crucial role at an individual level during MPMV RNA packaging and propagation.

Redundant role of SL3, Gag SL1, and Gag SL2 in MPMV RNA packaging and propagation

Redundancy is a common characteristic of retroviruses and it is possible that when deleting only one of the three stem loops (SL3, Gag SL1, and Gag SL2), the remaining stem loops compensate for the loss of the deleted stem loop for maintaining and stabilizing the major structural motifs of the 5′ UTR important for MPMV RNA packaging and propagation. To test this possibility, further mutants were created in which sequences involved in forming SL3, Gag SL1, and Gag SL2 were deleted or substituted simultaneously in multiple combinations. In mutant RK18, the same sequences that were deleted individually in RK15 (33 nts of SL3) and RK17 (39 nts of Gag SL1) were deleted simultaneously, creating a 72-nt discontinuous deletion mutant, removing most of SL3 and all of Gag SL1 (Fig. 1C). Employing a similar strategy, another double deletion mutant, RK19, was created in which sequences involved in forming SL3 and Gag SL2 were simultaneously deleted (a 63-nt discontinuous deletion mutant; Fig. 1C). Next, a third double-deletion mutant with a 69-nt discontinuous mutation was created, RK20, involving simultaneous deletion of Gag SL1 and Gag SL2 stem loops. To determine whether these stem loops could compensate for each other, a substitution mutant RK21 was created in which the sequences involved in forming Gag SL1 were exchanged with Gag SL2 sequences (Fig. 1C). Finally, the most drastic deletion mutant containing a 102-nt discontinuous deletion, RK22, was created in which sequences involved in forming all three stem loops (SL3, Gag SL1, and Gag SL2) were deleted simultaneously (Fig. 1C).

These double and triple deletion and substitution transfer vectors were also tested in the *in vivo* packaging and propagation assay, as described above. Results presented in Fig. 3A, panel V and 3B demonstrate that these transfer vector RNAs were stably expressed and exported to the cytoplasm despite these drastic deletions. Test of the packaging efficiency of the double-deletion mutant transfer vector RNAs relative to the wild type revealed that some of the mutants showed more pronounced effects than others, but did not completely abrogated RNA packaging (Fig. 3C). For example, RK18 (ΔSL3 and ΔGag SL1) showed the most drastic effect with a ~ 5-fold reduction in relative packaging efficiency (RPE = 0.23; p value = 3.00E-04) in comparison to RK19 (ΔSL3 & ΔGag SL2) and RK20 (ΔGag SL1 & ΔGag SL2, respectively). These latter mutants showed much better RPEs of 0.44 and 0.34, respectively (p values = 9.00E-04 and 2.30E-02; Fig. 3C). Interestingly, either double deletion of Gag SL1 and Gag SL2 (as in RK20), or exchange of the sequences forming these two stem loops in RK21, had a similar loss of RNA packaging (RPE of ~0.35 compared to the wild type; Fig. 3C). A more drastic impairment, but not complete abrogation, in RNA packaging was observed with the triple deletion mutant, RK22 (ΔSL3, Gag SL1, and Gag SL2) which showed a 10-fold reduction in RPE (0.11) when compared to the wild type, SJ2 (p value = 2.00E-05; Fig. 3C). The RNA packaging data of these mutants (RK19, RK20, RK21, and RK22) correlated well with the RNA propagation data (Fig. 3D). Such enhanced reduction but incomplete abrogation in both RNA packaging and propagation of some of the double deletion mutants and especially the triple deletion mutant, RK22, could partially be attributed to the rather large deletions in these vectors (63, 69, 72, and 102 nts, respectively). This is in contrast to our earlier work where only a few nucleotide deletion/substitution mutations in the two LRIs abrogated RNA packaging compared to the wild type [20]. For example, minimal substitution mutations that changed 4–5 G:U wobble pairs to G:C within the LRIs nearly abrogated RNA packaging [20], compared to the stem loop mutants in the present study that still retain RNA packaging despite deleting 30–102 nts, depending upon whether one, two, or three stem loops were deleted (Fig. 3C). Considering that these constructs were tested in a single round of replication assay which is highly sensitive for detecting small differences as the assay limits virus replication to one round with no possibility of reinfection, such

differences are probably biologically insignificant, if other replicative assays could be used.

Reduction in RNA packaging and propagation but not their total abrogation in multiple deletion/substitution mutants (RK18-RK22) further substantiates the data obtained from single deletion mutants (RK15-RK17) and confirms that sequences involved in forming these stem loops (SL3, Gag SL1, and Gag SL2) are not directly involved in RNA packaging. Additionally, since the principal packaging and dimerization determinants (such as pal SL, ssPurines, Region B, and part of Region A) lie outside this region, these stem loops may be important for stabilizing the structure of the 5′ UTR, perhaps in a redundant manner. Such a redundant role may be responsible for stabilizing the overall RNA structure of the region to ensure proper function that includes RNA packaging and dimerization. In summary, these observations suggest that sequences involved in forming the three tested stem loops had an effect on RNA packaging when tested in certain multiple combinations, but were not critical *per se* for the packaging potential of MPMV transfer vector RNAs.

Structure-function analyses of the mutant transfer vector RNAs

Since the structure of the 5′ end of the retroviral genome is critical for its functions, a detailed structure-function analysis of the tested mutants was conducted using hSHAPE chemical probing. Reactivity data was used as constraints in RNAStructure software [39], and for each mutant the more stable RNA secondary structure obtained (lower ΔG) was compared to the same region of the wild type structure in order to establish a relationship between the biological effects of the introduced mutation(s) and the RNA secondary structures.

Figure 4A shows the hSHAPE-validated structure of the wild type (SJ2) transfer vector RNA compared to that of the three single stem loop (SL3, Gag SL1, and Gag SL2) deletion mutants, RK15-RK17, which had a marginal effect on RNA packaging and propagation (Fig. 3C and D). The important sequence and structural motifs (stem loops) within this region, including PBS, pal SL, ssPurines, the two LRIs (I & II), and the three stem loops SL3, Gag SL1, and Gag SL2 are highlighted (Fig. 4A). Structural analyses of the deletion mutants revealed that the structure of pal SL and LRI-I & II, major functional motifs previously identified that have been shown to be important for RNA packaging and dimerization [15,19,20] remained essentially intact and similar to the wild type (Fig. 4B-D). Interestingly, in RK15, the ssPurine-rich region became partially base-paired due to the deletion of SL3, while Region B shown to be important for RNA packaging [19,22] re-folded into a new stem loop (Fig. 4B). This partial loss of ssPurines and/or re-folding of Region B may explain the slight reduction in packaging and propagation observed in this mutant (Fig. 3C and D), while six nucleotides within region 'B' [19] that are base paired in the wild type were partially located in a loop and lost their base pairing (Fig. 4B). Similarly, Gag SL2 in RK15, which is quite far from the deleted region, displayed an increased reactivity of its apical loop compared to the WT and absorbed the small stem loop located at the basal part of Gag SL2 (Fig. 4B). Interestingly, deletion of Gag SL2 in RK16 or Gag SL1 in RK17 did not have much effect on the overall folding of the entire region except for the disappearance of the deleted stem loop (Fig. 4C and D).

The double deletions which involved ΔSL3 with either ΔGag SL1 or ΔGag SL2 in separate mutants (RK18 and RK19, respectively) showed a more pronounced effect on RNA packaging and propagation when compared to the single stem loop mutants, RK15-RK17 (Fig. 3C and D). Structural analysis of these two mutants (RK18 and RK19) shown in Fig. 5 revealed the same changes as observed in RK15 where the ssPurine-rich region became partially base-paired, whereas the pal SL and the two LRIs remained intact, while the six nucleotides in region 'B' became single-stranded (Fig. 5B and C). Interestingly, the double deletion of SL3 and Gag SL1 in RK18 mutant lead to a new fold of Gag SL2, whereas double deletion of SL3 and Gag SL2 in RK19 did not affect Gag SL1 stem loop structure (Fig. 5B and C). In both these cases, the pal SL and the LRIs remained intact. Similarly, double deletion of Gag SL1 and Gag SL2 in RK20 resulted in a structure where the pal SL, ssPurines (regions critical for RNA packaging in MPMV), and LRIs remained folded nearly identical to wild type (Fig. 5D). The exchange between Gag SL1 and Gag SL2 in RK 21 on the other hand, resulted in partial base-pairing of ssPurines and refolding of Gag SL1, while the exchanged Gag SL2 maintained its native structure (Fig. 6B). Despite these differences between RK20 and RK21 structures, there was almost identical effects on RNA packaging and propagation observed in these mutants, even though RK20 had a deletion of 69 nucleotides, while RK21 was a substitution mutant (Fig. 5D *versus* 6B). These data confirm our earlier observation that Gag SL1 and Gag SL2 have minor effects on RNA packaging and these structures lie outside the principal packaging determinant of MPMV.

In the case of triple mutant, RK22, which involved simultaneous deletions of SL3, Gag SL1, and Gag SL2, the RNA packaging and propagation were further reduced (Fig. 3C, D). Consistent with secondary structures of RK15, RK18, and RK19 (Figs. 4B, 5B and C), the mutants where SL3 was deleted either alone or in combination with other stem loops, the ssPurine-rich region became partially base paired in RK22 as well, while maintaining the pal SL and the LRIs (Fig. 6C). These results suggest that deletion of SL3 contributes to the partial base pairing of the ssPurine-rich region and perhaps to the restructuring of Gag SL2 stem loop (mutants RK15, RK18, RK19, and RK22 *versus* WT SJ2). Based on these analyses, we conclude that as long as the two LRIs, pal SL, and some parts of ssPurine-rich region are maintained, deletion of any of the three tested stem loops was dispensable for both RNA packaging and propagation of MPMV transfer vectors RNAs. However, since simultaneous deletion of the three stem loops (SL3, Gag SL1, Gag SL2) showed more pronounced effect on RNA packaging (~10 fold less compared to wild type while still maintaining the two LRIs, pal SL, and some part of ssPurine-rich region), this suggests that the sequences involved in forming these stem loops may have an indirect effect by maintaining the overall stability of this structured region. Further evidence of the existence of such a stabilizing effect is the link we

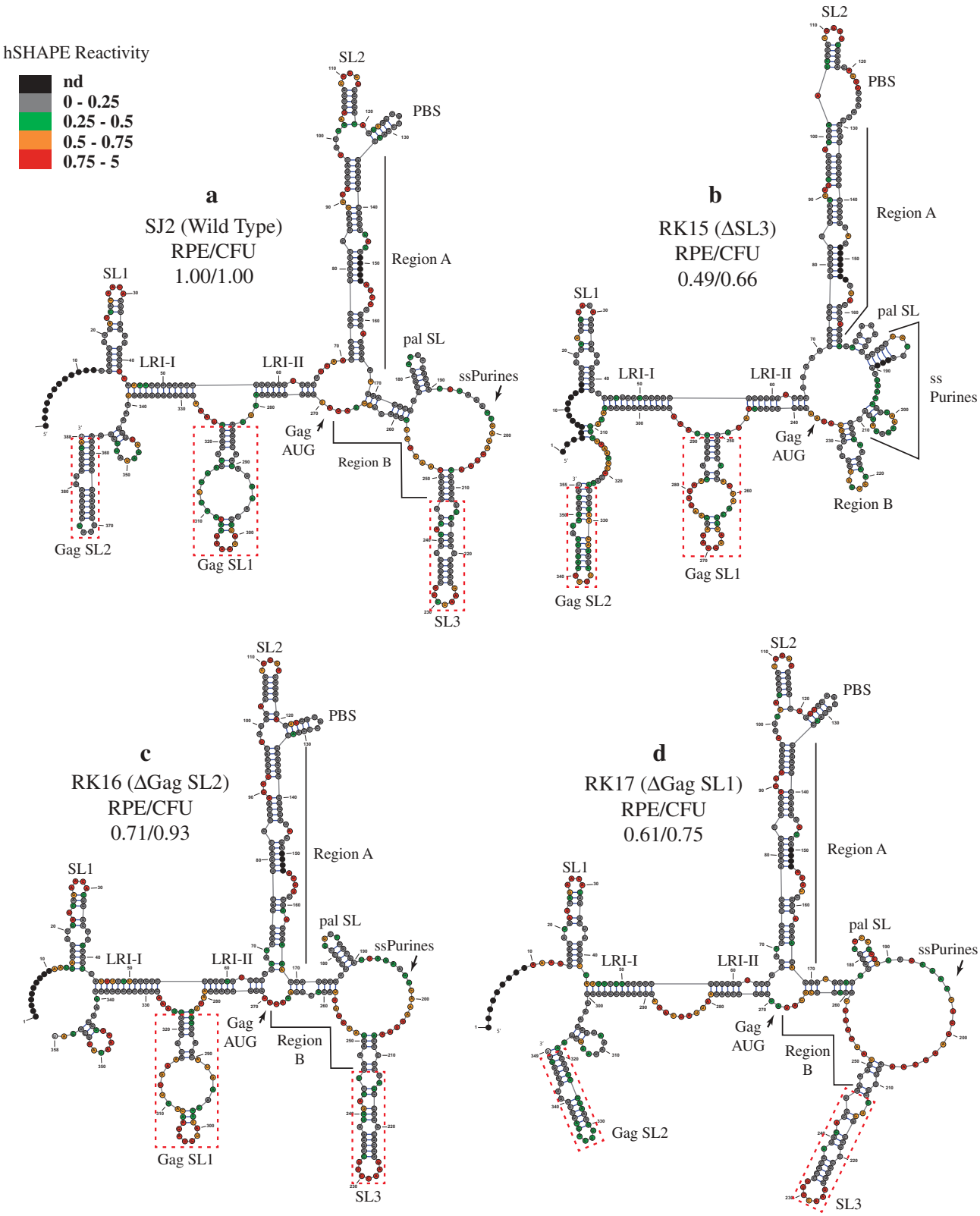

Figure 4. hSHAPE-validated secondary structures of the mutant transfer vector packaging signal RNAs containing individual deletions of SL3, Gag SL1, and Gag SL2. (a) MPMV wild type transfer vector SJ2, **(b)** RK15 containing a deletion of SL3, **(c)** RK16 mutant transfer vector containing a deletion of Gag SL2, and **(d)** RK17 mutant transfer vector containing a deletion of Gag SL1. The SHAPE reactivities are an average of three independent experiments and were applied to RNAstructure program and the structure with the least minimum free energy was selected. Nucleotides are color annotated as per the SHAPE reactivities key shown. The SHAPE analyzed structures were redrawn using Structure Editor program with the major structural elements highlighted.

identified between the deletion of SL3 and/or the partial pairing of ssPurine-rich region and the misfold of Gag SL2. This scenario is similar to the early reports on HIV TAR that suggested TAR as having a role in genomic RNA packaging

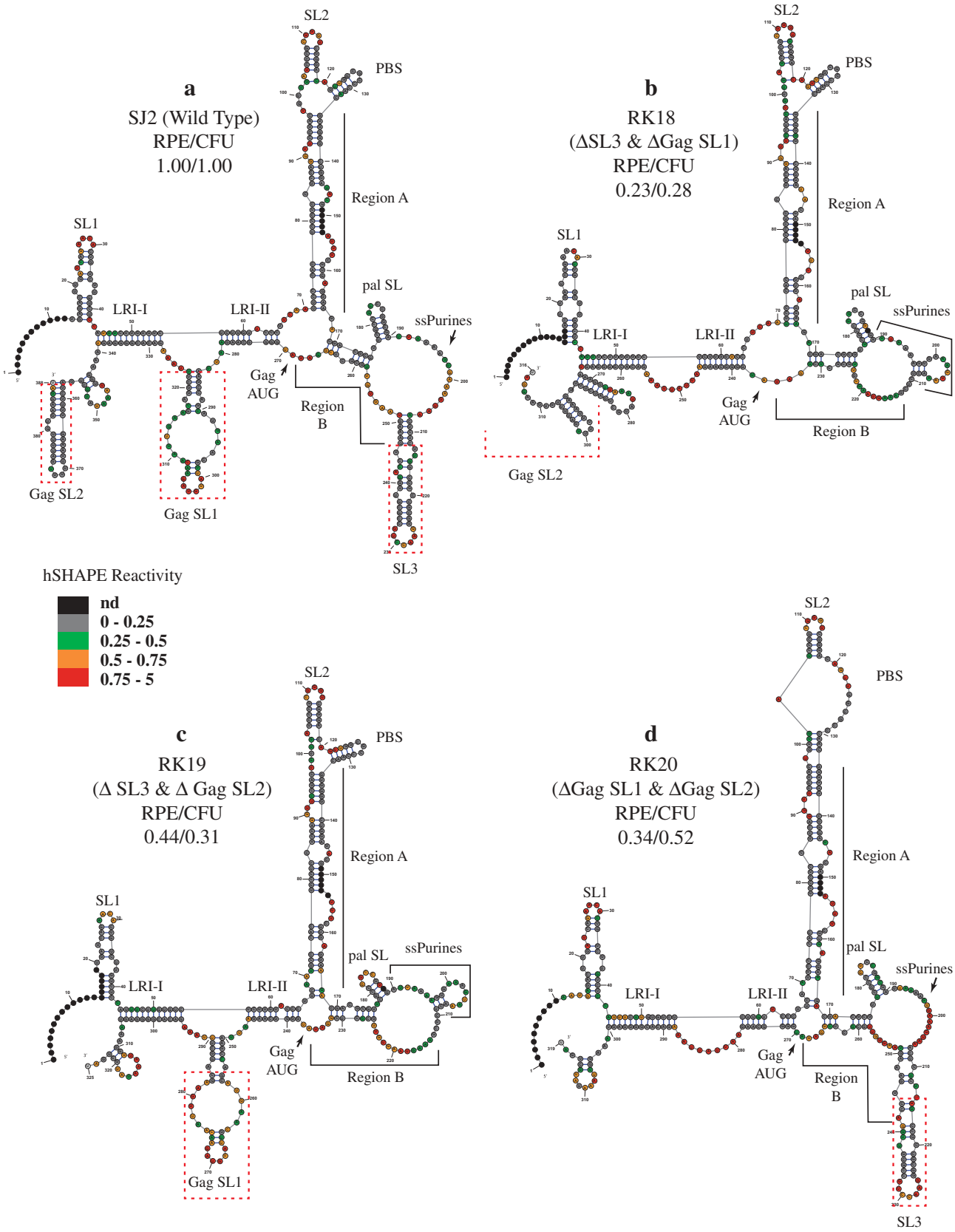

Figure 5. hSHAPE-validated secondary structures of the mutant transfer vector packaging signal RNAs containing multiple deletions/substitutions of SL3, Gag SL1, and Gag SL2. (a) MPMV wild type transfer vector SJ2, **(b)** RK18 containing a double deletion of SL3 and Gag SL1, **(c)** RK19 mutant transfer vector containing a double deletion of SL3 and Gag SL2, and **(d)** RK20 mutant transfer vector containing a double deletion of Gag SL1 and Gag SL2. The SHAPE reactivities are an average of three independent experiments and were applied to RNAstructure program and the structure with the least minimum free energy was selected. Nucleotides are color annotated as per the SHAPE reactivities key shown. The SHAPE analyzed structures were redrawn using Structure Editor program with the major structural elements highlighted.

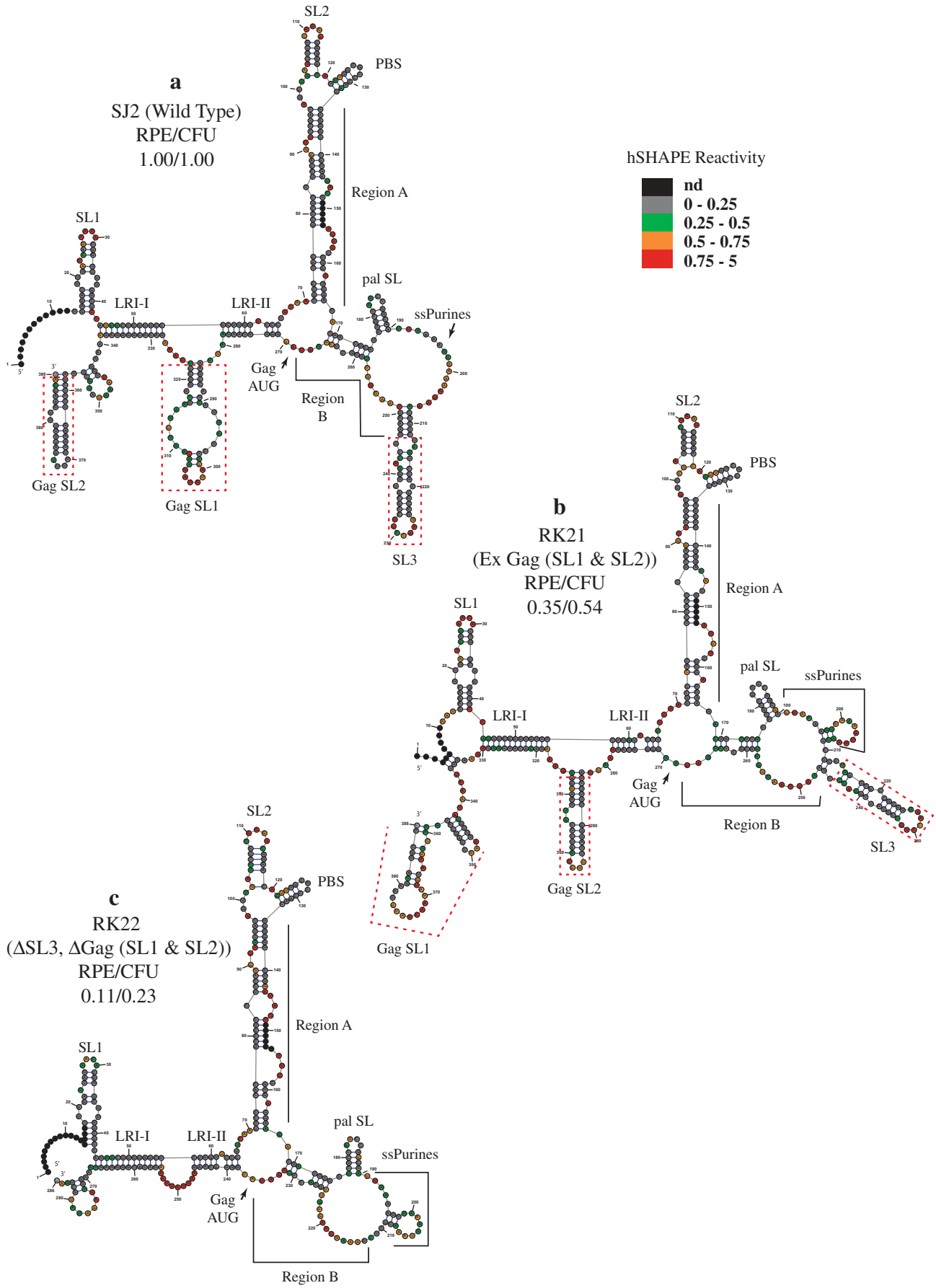

Figure 6. hSHAPE-validated secondary structures of the mutant transfer vector packaging signal RNAs containing exchange or triple deletions of SL3, Gag SL1, and Gag SL2. (a) MPMV wild type transfer vector SJ2, **(b)** RK21 mutant transfer vector containing an exchange of Gag SL1 with Gag SL2, and **(c)** RK22 mutant transfer vector containing a triple deletion of SL3, Gag SL1, and Gag SL2. The SHAPE reactivities are an average of three independent experiments and were applied to RNAstructure program and the structure with the least minimum free energy was selected. Nucleotides are color annotated as per the SHAPE reactivities key shown. The SHAPE analyzed structures were redrawn using Structure Editor program with the major structural elements highlighted.

[40–45]. Later experiments clarified that destabilization of the TAR structural element led to a global RNA refolding affecting motifs that were important in RNA packaging, dimerization, or polyadenylation [46]. Thus, TAR had a more indirect role in RNA packaging by 'stabilizing' the region with no direct role itself in the process of gRNA packaging by the virus.

It is interesting to note that the sequences forming SL3, which are found in close vicinity of the ssPurine-rich region (a motif critical for RNA packaging), were not important since its deletion in RK15 only marginally affected RNA packaging or propagation (Fig. 3C and D). This agrees with our previous systematic deletion analysis of the 5′ UTR sequences of MPMV that showed that a specific 35-nucleotide deletion that removed most of SL3, had limited effect on RNA packaging [19]. Together, structural analyses of the single and multiple deletion mutants (RK15-RK20) support an indirect structural role of the SL3 sequences in MPMV genomic RNA packaging, as has been proposed previously [19].

Unlike most retroviruses with one identified LRI, MPMV contains two LRIs (LRI-I and LRI-II; Fig. 1) both of which maintain the interaction between U5 and *gag* sequences [30,31,33,34,47,48]. These two LRIs have been shown to play architectural role in stabilizing the RNA secondary structure of the 5′ UTR sequences that are important for MPMV RNA packaging [20]. Based on the organization of the SHAPE-validated structure, it is reasonable to theorize that while LRIs stabilize 5′ UTR sequences, the overall RNA secondary structure is further spatially held together by the three stem loops (SL3, Gag SL1, and Gag SL2) comprising of sequences from the distal parts of the 5′ UTR and *gag* (Fig. 1A). Since these stem loops, either individually or in multiples, were observed to be dispensable for RNA packaging and propagation (Fig. 3C and D), our results further suggest that the MPMV packaging signal RNA secondary structure can potentially be separated into two parts that are held together by U5-Gag LRIs: the upper part of the structure comprising of several structural motifs (the dimerization initiation site (DIS), pal SL and ssPurine-rich region) that either have been shown or proposed to be important for MPMV RNA packaging and dimerization [15,19,20,22], and the lower part of the structure containing the three stem loops (SL3, Gag SL1, and Gag SL2), that perhaps serve to provide further architectural support to the overall RNA secondary structure during the process of RNA packaging and dimerization.

It is well-known that retroviral gRNA packaging determinants involve sequences present at the 5′end of *gag* as well [1–3,5–7,9]; however, their precise contribution to retroviral RNA packaging has remained largely elusive. Recent deletion analyses as well as biochemical validation of the packaging determinants and higher order structures in various retroviruses such as HIV, FIV, MMTV, and MPMV suggest that the role of *gag* sequences (especially proximal to the *gag* AUG) is primarily due to their involvement in forming LRIs with sequences in the R/U5 region [15,20,30,31,33,34,47–50]. For example, in the case of FIV, initially ~100–230 nts of FIV *gag* were shown to be required for optimally packaging gRNA into viral particles [35,51–53]. Subsequent deletion analysis of FIV *gag* sequences revealed that deletion of only the proximal 13 nts of *gag* could severely impair RNA packaging [54]. It was later observed that 7 out of these 13 nts were involved in forming an LRI between U5 and *gag* sequences [30] and subsequent studies confirmed the biological existence and significance of such U5-Gag LRI in FIV RNA packaging [31,33]. In the case of HIV-1, a recent study further emphasizes this showing that efficient encapsidation of a heterologous RNA into viral particles requires *gag* sequences flanking the AUG, presumably for LRI interactions with U5 [55]. Similarly, in MMTV, even though 120 nts within *gag* have been reported to be required for efficient RNA encapsidation, later studies suggested that the first 30 nts are absolutely required out of which the first 15 nts are involved in LRI interactions with U5 [34,37]. These observations suggest a crucial role of proximal *gag* sequences in RNA packaging via the formation of LRI(s), but in turn raise the question of what could be the role of the distal part of the *gag* sequences in RNA packaging.

Other than their involvement in LRIs to stabilize the packaging signal RNA secondary structure, *gag* sequences may have some other important roles. For example, in bovine leukemia virus (BLV), it is clear that part of the packaging signal sequence lies within *gag* as an RNA structural element [56,57]. In the case of FIV, *gag* sequences may be important for gRNA dimerization since the biochemically- and biologically-validated RNA secondary structure of the packaging signal RNA contains a palindrome in the proximal part of *gag* that functions as the DIS for FIV gRNA dimerization [30,31]. This conferring high specificity packaging, limited exclusively to the unspliced viral RNA, especially if it is assumed that gRNA packaging is dependent on the recognition of a dimeric RNA, as is usually the case in retroviruses [4,8,58]. However, the answer is not so clear for other retroviruses. For example, in other retroviruses, in addition to gRNA dimerization, it is speculated that *gag* sequences may also be facilitating interaction of Gag polyprotein precursor with the Gag-binding domains within the packaging signal RNA structure itself [59]. This could be via the *gag* AUG/U5 interactions acting as a structural switch to open the Gag-binding domains on the packaging signal RNA, as has been suggested for HIV-1 [47,50,60] and MLV [61,62]. Thus, it is possible that in the case of MPMV, occlusion of the *gag* AUG by the LRIs themselves may act as a temporal switch between translation of the full-length RNA *versus* RNA packaging [20].

Furthermore, comparative analysis of the predicted unspliced genomic and spliced envelope (Env) MPMV mRNAs has shown that the pal SL and ssPurines loops (critical for RNA dimerization and packaging, respectively) become fully base paired (pal SL) or partially base paired (ssPurines) in the spliced Env mRNA [15]. The refolding of these important packaging determinants in the spliced Env mRNA suggests their potential limiting ability to perform RNA-RNA or RNA-protein interactions. A similar observation has been made in the case of MMTV, another *betaretrovirus*, where both the DIS and ssPurines found in an open single-stranded conformation in the gRNA [34] are base paired in the Env and Sag spliced mRNAs (unpublished observations). The fact that the two LRIs in MPMV and the LRI in MMTV are located downstream of the mSD and therefore exclusively present in the gRNA (Fig. 1 [15,34]), suggests that *gag* sequences may not only be involved in the structural stability of the packaging signal RNA, but also

specificity of the gRNA as a substrate for encapsidation into the progeny virion.

In summary, our results reveal that the 5′end of the MPMV gRNA is held together by two U5-Gag LRIs that have a more important architectural role in stabilizing the structure of the MPMV 5′ UTR than the more distal 5′ UTR and *gag* sequences involved in forming SL3, Gag SL1, and Gag SL2. These distal stem loops perhaps help maintain the proper folding and stability of the overall RNA secondary structure for function, even though none of these by themselves are directly involved in the MPMV RNA packaging process. The data presented here enhance our understanding of the molecular intricacies involved during the MPMV RNA packaging and dimerization processes and further shed light on the role of *gag* sequences in the packaging process.

Material and methods

Nucleotide numbering system

Nucleotide numbers in the study correspond to the MPMV genome with the Genbank accession number M12349 [23].

Construction of plasmids

TR301 is the MPMV Gag/Pol packaging construct, MD.G is the vesicular stomatitis virus glycoprotein G (VSV-G) expression vector, and SJ2 is the wild type MPMV sub-genomic transfer vector that have been described previously [19,35,36] (Fig. 2). SJ2 expresses the *hygromycin B phosphotransferase* selectable marker from an internal simian virus 40 early promoter (SV-Hyg^r) to monitor the effect of the mutations on propagation of the packaged viral RNA (Fig. 1B).

The deletion and substitution mutations were introduced using splice overlap extension (SOE) PCR using the wild type vector, SJ2, as a template, as described previously [20]. Briefly, it required two rounds of amplifications: the first-round amplification comprised of two separate reactions, A and B in which PCR (A) was conducted using the common outer (forward or sense; S) oligo OTR787, **Table S1**) along with the inner (or antisense; AS) oligo that was specific for each mutation being introduced (**Table S1**). PCR B was performed using the AS outer primer OTR788 (**Table S1**) in combination with an inner S primer that was also specific for each mutation that was being introduced (**Table S1**). The amplified products from these two independent reactions (PCR A and PCR B) harbor complementary sequences allowing them to anneal, resulting in a template with the desired mutation for round 2 PCR amplification which was performed using outer S and AS primers (OTR787/OTR788; **Table S1**), generating a final PCR product containing the desired mutation. The final PCR- products containing the desired mutations were digested with *Xho*I and *BamH*I restriction enzymes and cloned into wild type transfer vector, SJ2 replacing the region in which mutations have been introduced. The sequence of all mutant clones was verified by DNA sequencing. Sequences of primers used for the PCR and cloning are listed in **Table S1**.

Nucleocytoplasmic fractionation, RNA isolation, and cDNA preparation

Cytoplasmic and nuclear fractions were prepared from the transfected cells as described earlier [19,20,32,33,63]. RNA preparations were tested for the presence of any residual contaminating plasmid DNA using MPMV specific primer pair: OTR 1161 and OTR 1163 (**Table S1**) as described earlier [20]. After having confirmed the lack of any plasmid DNA contamination, RNA preparations were reverse transcribed and used for further analyses, as described earlier [20].

Estimation of relative packaging efficiency (RPE)

The relative expression of transfer vector RNAs in the cytoplasm and their packaging efficiency into the virus particles was quantified using the custom-made Taqman gene expression assay (Applied Biosystems Inc., ABI) used earlier to determine the significance of LRIs to MPMV RNA packaging [20]. Briefly, this assay consisted of unlabeled primers and a FAM/MGB-labeled probe in MPMV U5/PBS region identical in both the wild type and mutant transfer vector RNAs, but away from the site of the introduced mutations. The region amplified was upstream of the major splice donor of MPMV, and does not contain any known splice sites in the wild type or mutant transfer vectors, including the SV-Hyg^r cassette, making it unlikely that aberrant splicing could result in the generation of spliced RNAs. We have previously used this vector design successfully for monitoring gRNA packaging [19,20,22,35]. Furthermore, results obtained from *in vivo* RNA packaging assay have correlated well with the RNA propagation data obtained in an independent manner by measuring the counts of hygromycin-resistant colonies (CFU/ml) observed after transduction of the infected cells with pseudotyped-virions containing packaged wild type and mutant RNAs [20].

To allow relative quantification, a pre-designed VIC/MGB-labelled human β-actin assay (ABI #4326315E) was used as described previously [20]. The assay was conducted using equal amounts of cDNAs from the wild type and mutant samples that were amplified for 50 cycles in triplicates for both MPMV and β-actin targets using the ABI QuantStudio 7 (ABI, CA, USA). To control for differences in transfection efficiencies, the relative quantification (RQ) values obtained for MPMV cytoplasmic expression was further normalized to the luciferase values obtained per μg protein. Packaging efficiency was thus estimated by dividing the results obtained for MPMV expression in the virions by those for the cytoplasmic expression reported relative to the wild type levels.

MPMV RNA structure probing by hSHAPE

In order to correlate the effects of the introduced mutations in the MPMV packaging signal RNA with their secondary structure, the 5′end of the wild type and mutant transfer vector RNAs (region between R and the first 120 nts of *gag*) were subjected to hSHAPE chemical probing [64–66] following the protocol described previously [15,20,34,38]. Briefly, *in vitro* transcribed RNAs were folded in a buffer favoring gRNA

dimerization (50 mM sodium cacodylate (pH 7.5), 300 mM KCl and 5 mM $MgCl_2$) and modified with benzoyl cyanide (BzCN) in the presence of 2 µg total yeast tRNA (Sigma Aldrich). The modified RNAs were reverse transcribed using AS primers 1 and 2: (5′-AGT TAC TGG GAC TTT CTC CG-3′; MPMV nt 483–502 relative to WT) labelled with VIC or NED, respectively, and AS primers 3 and 4: (5′- CTT ACT TTC AGG TCC AAC CG –3′; MPMV nt 235–234 relative to WT) labelled with VIC or NED. These primers allowed analysis of the RNA structure from ~ nucleotide 450 to 10. The primer extension products were loaded onto an Applied Biosystems 3130xl Genetic Analyzer and the electropherograms were analyzed with the QuShape software [67]. The hSHAPE reactivities obtained with QuShape from three independent experiments were averaged (**Table S2**) before being used as constraints to fold the RNA secondary structure of the MPMV packaging signal with the RNAstructure software version 6.0 [39] to determine the effects of mutations on the overall higher order structure. Based on the RNAstructure data, the structure of WT and mutants RNAs were drawn using the Structure Editor graphical tool, a module of the RNAstructure software.

Statistical analysis

For quantitation and determination of statistically significant differences in relative packaging efficiencies between the wild type and mutant clones, the standard paired, two-tailed Students *t*-test was performed. A *p*-value of <1.00E-3 was considered statistically significant in the RNA packaging assays, while a *p*-value of 1.00E-2 was considered significant for the propagation assays.

Disclosure of Potential Conflicts of Interest

No potential conflicts of interest were disclosed

Funding

This research was funded primarily by a grant from the United Arab Emirates University (UAEU) Program for Advanced Research-UPAR (31M131) and in part by a grant from the College of Medicine and Health Sciences (NP/12/43) to TAR, and United Arab Emirates University (UAEU) grants 31M122 and 31R122 to FM.

ORCID

Valérie Vivet-Boudou http://orcid.org/0000-0001-8702-1047
Farah Mustafa http://orcid.org/0000-0002-1081-3756

References

[1] Ali LM, Rizvi TA, Mustafa F. Cross- and co-packaging of retroviral RNAs and their consequences. Viruses. 2016;8(10).
[2] Comas-Garcia M, Davis SR, Rein A. On the selective packaging of genomic RNA by HIV-1. Viruses. 2016;8(9):246.
[3] D'Souza V, Summers MF. How retroviruses select their genomes. Nat Rev Microbiol. 2005;3(8):643–655.
[4] Dubois N, Marquet R, Paillart J-C, et al. Retroviral RNA dimerization: from structure to functions. Front Microbiol. 2018;9:527.
[5] Johnson SF, Telesnitsky A. Retroviral RNA dimerization and packaging: the what, how, when, where, and why. PLoS Pathog. 2010;6(10):e1001007.
[6] Kaddis Maldonado RJ, Parent LJ. Orchestrating the selection and packaging of genomic RNA by retroviruses: an ensemble of viral and host factors. Viruses. 2016;8(9):257.
[7] Lever AM. HIV-1 RNA packaging. Adv Pharmacol. 2007;55:1–32.
[8] Paillart JC, Shehu-Xhilaga M, Marquet R, et al. Dimerization of retroviral RNA genomes: an inseparable pair. Nat Rev Microbiol. 2004;2(6):461–472.
[9] Mailler E, Bernacchi S, Marquet R, et al. The life-cycle of the HIV-1 Gag-RNA complex. Viruses. 2016;8(9).
[10] Bryant ML, Gardner MB, Marx PA, et al. Immunodeficiency in rhesus monkeys associated with the original Mason-Pfizer monkey virus. J Natl Cancer Inst. 1986;77(4):957–965.
[11] Fine DL, Landon JC, Pienta RJ, et al. Responses of infant rhesus monkeys to inoculation with Mason-Pfizer monkey virus materials. J Natl Cancer Inst. 1975;54(3):651–658.
[12] Daniel MD, King NW, Letvin NL, et al. A new type D retrovirus isolated from macaques with an immunodeficiency syndrome. Science. 1984;223(4636):602–605.
[13] Desrosiers RC, Daniel MD, Butler CV, et al. Retrovirus D/New England and its relation to Mason-Pfizer monkey virus. J Virol. 1985;54(2):552–560.
[14] Marx PA, Maul DH, Osborn KG, et al. Simian AIDS: isolation of a type D retrovirus and transmission of the disease. Science. 1984;223(4640):1083–1086.
[15] Aktar SJ, Jabeen A, Lm A, et al. SHAPE analysis of the 5′ end of the Mason-Pfizer monkey virus (MPMV) genomic RNA reveals structural elements required for genome dimerization. Rna. 2013;19(12):1648–1658.
[16] Bray M, Prasad S, Dubay JW, et al. A small element from the Mason-Pfizer monkey virus genome makes human immunodeficiency virus type 1 expression and replication Rev-independent. Proc Natl Acad Sci USA. 1994;91(4):1256–1260.
[17] Guesdon FM, Greatorex J, Rhee SR, et al. Sequences in the 5' leader of Mason-Pfizer monkey virus which affect viral particle production and genomic RNA packaging: development of MPMV packaging cell lines. Virology. 2001;288(1):81–88.
[18] Harrison GP, Hunter E, Lever AM. Secondary structure model of the Mason-Pfizer monkey virus 5′ leader sequence: identification of a structural motif common to a variety of retroviruses. J Virol. 1995;69(4):2175–2186.
[19] Jaballah SA, Aktar SJ, Ali J, et al. A G-C-rich palindromic structural motif and a stretch of single-stranded purines are required for optimal packaging of Mason-Pfizer monkey virus (MPMV) genomic RNA. J Mol Biol. 2010;401(5):996–1014.
[20] Kalloush RM, Vivet-Boudou V, Ali LM, et al. Packaging of Mason-Pfizer monkey virus (MPMV) genomic RNA depends upon conserved long-range interactions (LRIs) between U5 and gag sequences. Rna. 2016;22(6):905–919.
[21] Mustafa F, Lew KA, Schmidt RD, et al. Mutational analysis of the predicted secondary RNA structure of the Mason-Pfizer monkey virus packaging signal. Virus Res. 2004;99(1):35–46.
[22] Schmidt RD, Mustafa F, Lew KA, et al. Sequences within both the 5′ untranslated region and the gag gene are important for efficient encapsidation of Mason-Pfizer monkey virus RNA. Virology. 2003;309(1):166–178.
[23] Sonigo P, Barker C, Hunter E, et al. Nucleotide sequence of Mason-Pfizer monkey virus: an immunosuppressive D-type retrovirus. Cell. 1986;45(3):375–385.
[24] Vile RG, Ali M, Hunter E, et al. Identification of a generalised packaging sequence for D-type retroviruses and generation of a D-type retroviral vector. Virology. 1992;189(2):786–791.
[25] Rizvi TA, Lew KA, Murphy EC, et al. Role of Mason-Pfizer monkey virus (MPMV) constitutive transport element (CTE) in the propagation of MPMV vectors by genetic complementation using homologous/heterologous env genes. Virology. 1996;224(2):517–532.

[26] Rizvi TA, Schmidt RD, Lew KA. Mason-Pfizer monkey virus (MPMV) constitutive transport element (CTE) functions in a position-dependent manner. Virology. 1997;236(1):118–129.
[27] Rizvi TA, Schmidt RD, Lew KA, et al. Rev/RRE-independent Mason-Pfizer monkey virus constitutive transport element-dependent propagation of SIVmac239 vectors using a single round of replication assay. Virology. 1996;222(2):457–463.
[28] Baudin F, Marquet R, Isel C, et al. Functional sites in the 5′ region of human immunodeficiency virus type 1 RNA form defined structural domains. J Mol Biol. 1993;229(2):382–397.
[29] Rizvi TA, Panganiban AT. Simian immunodeficiency virus RNA is efficiently encapsidated by human immunodeficiency virus type 1 particles. J Virol. 1993;67(5):2681–2688.
[30] Kenyon JC, Ghazawi A, Cheung WKS, et al. The secondary structure of the 5′ end of the FIV genome reveals a long-range interaction between R/U5 and gag sequences, and a large, stable stem-loop. Rna. 2008;14(12):2597–2608.
[31] Kenyon JC, Tanner SJ, Legiewicz M, et al. SHAPE analysis of the FIV Leader RNA reveals a structural switch potentially controlling viral packaging and genome dimerization. Nucleic Acids Res. 2011;39(15):6692–6704.
[32] Mustafa F, Ghazawi A, Jayanth P, et al. Sequences intervening between the core packaging determinants are dispensable for maintaining the packaging potential and propagation of feline immunodeficiency virus transfer vector RNAs. J Virol. 2005;79(21):13817–13821.
[33] Rizvi TA, Kenyon JC, Ali J, et al. Optimal packaging of FIV genomic RNA depends upon a conserved long-range interaction and a palindromic sequence within gag. J Mol Biol. 2010;403(1):103–119.
[34] Aktar SJ, Vivet-Boudou V, Ali LM, et al. Structural basis of genomic RNA (gRNA) dimerization and packaging determinants of mouse mammary tumor virus (MMTV). Retrovirology. 2014;11:96.
[35] Browning MT, Schmidt RD, Lew KA, et al. Primate and feline lentivirus vector RNA packaging and propagation by heterologous lentivirus virions. J Virol. 2001;75(11):5129–5140.
[36] Naldini L, Blömer U, Gallay P, et al. In vivo gene delivery and stable transduction of nondividing cells by a lentiviral vector. Science. 1996;272(5259):263–267.
[37] Mustafa F, Al Amri D, Al Ali F, et al. Sequences within both the 5′ UTR and Gag are required for optimal in vivo packaging and propagation of mouse mammary tumor virus (MMTV) genomic RNA. PLoS One. 2012;7(10):e47088.
[38] Mustafa F, Vivet-Boudou V, Jabeen A, et al. The bifurcated stem loop 4 (SL4) is crucial for efficient packaging of mouse mammary tumor virus (MMTV) genomic RNA. RNA Biol. 2018;15(8):1047–1059.
[39] Reuter JS, Mathews DH, Mustafa F, et al. RNAstructure: software for RNA secondary structure prediction and analysis. BMC Bioinformatics. 2010;11:129.
[40] Berkhout B. Multiple biological roles associated with the repeat (R) region of the HIV-1 RNA genome. Adv Pharmacol. 2000;48:29–73.
[41] Clever JL, Miranda D Jr., Parslow TG. RNA structure and packaging signals in the 5' leader region of the human immunodeficiency virus type 1 genome. J Virol. 2002;76(23):12381–12387.
[42] Das AT, Harwig A, Vrolijk MM, et al. The TAR hairpin of human immunodeficiency virus type 1 can be deleted when not required for Tat-mediated activation of transcription. J Virol. 2007;81(14):7742–7748.
[43] Das AT, Klaver B, Berkhout B. The 5′ and 3′ TAR elements of human immunodeficiency virus exert effects at several points in the virus life cycle. J Virol. 1998;72(11):9217–9223.
[44] Helga-Maria C, Hammarskjold ML, Rekosh D. An intact TAR element and cytoplasmic localization are necessary for efficient packaging of human immunodeficiency virus type 1 genomic RNA. J Virol. 1999;73(5):4127–4135.
[45] McBride MS, Schwartz MD, Panganiban AT. Efficient encapsidation of human immunodeficiency virus type 1 vectors and further characterization of cis elements required for encapsidation. J Virol. 1997;71(6):4544–4554.
[46] Das AT, Vrolijk MM, Harwig A, et al. Opening of the TAR hairpin in the HIV-1 genome causes aberrant RNA dimerization and packaging. Retrovirology. 2012;9:59.
[47] Abbink TE, Berkhout B. A novel long distance base-pairing interaction in human immunodeficiency virus type 1 RNA occludes the Gag start codon. J Biol Chem. 2003;278(13):11601–11611.
[48] Paillart JC, Skripkin E, Ehresmann B, et al. In vitro evidence for a long range pseudoknot in the 5′-untranslated and matrix coding regions of HIV-1 genomic RNA. J Biol Chem. 2002;277(8):5995–6004.
[49] Nikolaitchik O, Rhodes TD, Ott D, et al. Effects of mutations in the human immunodeficiency virus type 1 Gag gene on RNA packaging and recombination. J Virol. 2006;80(10):4691–4697.
[50] Lu, K., et al. NMR detection of structures in the HIV-1 5′-leader RNA that regulate genome packaging. Science. 2011;334(6053):242–245.
[51] Browning MT, Mustafa F, Schmidt RD, et al. Sequences within the gag gene of feline immunodeficiency virus (FIV) are important for efficient RNA encapsidation. Virus Res. 2003;93(2):199–209.
[52] Browning MT, Mustafa F, Schmidt RD, et al. Delineation of sequences important for efficient packaging of feline immunodeficiency virus RNA. J Gen Virol. 2003;84(Pt 3):621–627.
[53] Poeschla EM, Wong-Staal F, Looney DJ. Efficient transduction of nondividing human cells by feline immunodeficiency virus lentiviral vectors. Nat Med. 1998;4(3):354–357.
[54] Kemler I, Azmi I, Poeschla EM. The critical role of proximal gag sequences in feline immunodeficiency virus genome encapsidation. Virology. 2004;327(1):111–120.
[55] Liu Y, Nikolaitchik OA, Rahman SA, et al. HIV-1 sequence necessary and sufficient to package non-viral RNAs into HIV-1 particles. J Mol Biol. 2017;429(16):2542–2555.
[56] Mansky LM, Krueger AE, Temin HM. The bovine leukemia virus encapsidation signal is discontinuous and extends into the 5′ end of the gag gene. J Virol. 1995;69(6):3282–3289.
[57] Mansky LM, Wisniewski RM. The bovine leukemia virus encapsidation signal is composed of RNA secondary structures. J Virol. 1998;72(4):3196–3204.
[58] Greatorex J. The retroviral RNA dimer linkage: different structures may reflect different roles. Retrovirology. 2004;1:22.
[59] Bernacchi S, Abd El-Wahab EW, Dubois N, et al. HIV-1 Pr55 (Gag) binds genomic and spliced RNAs with different affinity and stoichiometry. RNA Biol. 2017;14(1):90–103.
[60] Abbink TE, Ooms M, Haasnoot PCJ, et al. The HIV-1 leader RNA conformational switch regulates RNA dimerization but does not regulate mRNA translation. Biochemistry. 2005;44(25):9058–9066.
[61] D'Souza V, Summers MF. Structural basis for packaging the dimeric genome of Moloney murine leukaemia virus. Nature. 2004;431(7008):586–590.
[62] Gherghe C, Lombo T, Leonard CW, et al. Definition of a high-affinity Gag recognition structure mediating packaging of a retroviral RNA genome. Proc Natl Acad Sci USA. 2010;107(45):19248–19253.
[63] Ghazawi A, Mustafa F, Phillip PS, et al. Both the 5′ and 3′ LTRs of FIV contain minor RNA encapsidation determinants compared to the two core packaging determinants within the 5′ untranslated region and gag. Microbes Infect. 2006;8(3):767–778.
[64] Merino EJ, Wilkinson KA, Coughlan JL, et al. RNA structure analysis at single nucleotide resolution by selective 2′-hydroxyl acylation and primer extension (SHAPE). J Am Chem Soc. 2005;127(12):4223–4231.
[65] Mortimer SA, Weeks KM. A fast-acting reagent for accurate analysis of RNA secondary and tertiary structure by SHAPE chemistry. J Am Chem Soc. 2007;129(14):4144–4145.
[66] Mortimer SA, Weeks KM. Time-resolved RNA SHAPE chemistry: quantitative RNA structure analysis in one-second snapshots and at single-nucleotide resolution. Nat Protoc. 2009;4(10):1413–1421.
[67] Karabiber F, McGinnis JL, Favorov OV, et al. QuShape: rapid, accurate, and best-practices quantification of nucleic acid probing information, resolved by capillary electrophoresis. Rna. 2013;19(1):63–73.
[68] Pitchai FNN, Ali L, Pillai VN, et al. Expression, purification, and characterization of biologically active full-length Mason-Pfizer monkey virus (MPMV) Pr78(Gag). Sci Rep. 2018;8(1):11793.